# Blocking TNFα-driven astrocyte purinergic signaling restores normal synaptic activity in epilepsy

Running title: TNFα controls astrocyte signaling in epilepsy

Ljiljana Nikolic[1‡], Weida Shen[1‡], Paola Nobili[1], Anaïs Virenque[2], Lauriane Ulmann[2], Etienne Audinat[1, 2 *]

[1]Neuron-glia interactions group, INSERM U1128, Paris Descartes University, Paris, France

[2] IGF, University of Montpellier, CNRS, INSERM, Montpellier, France

[‡]These authors contributed equally

[*]Correspondence: Etienne Audinat

e-mail address: etienne.audinat@igf.cnrs.fr

Institut de Génomique Fonctionnelle, CNRS UMR 5203, INSERM U1191

Université de Montpellier, 141 rue de la Cardonille, 34094 Montpellier Cedex 5, France

**Competing interests:** The authors declare no competing interests.

## Acknowledgments

We thank Peter Bedner and Christian Steinhäuser for their help with the mouse model of temporal lobe epilepsy, Frank Pfrieger for providing the Cx30-CreERT2 mice. We thank Serge Charpak for the access to the two-photon microscope, for fruitful discussions and for critical reading of an earlier version of the manuscript. We thank Yannick Goulam for his help with two-photon imaging, Amelyne David, Manon Omnes and Quentin Ferrari for maintaining the mouse colonies and genotyping the animals. Confocal pictures were acquired at the microscopy platform of the Saints Pères University Center. This work was supported by grants from the Fondation pour la Recherche Médicale (FRM: DEQ20140329488), the European Union (ERA-NET Neuron BrIE) and the Agence National de la Recherche (ANR-2011-BSV4-004-02). The Audinat lab is affiliated to Paris School of Neuroscience (ENP). WS was supported by a scholarship of the China Scholarship Council.

## Conflict of Interest Statement

The authors declare no conflict of interest.

## Word count:

Total: 4758

Introduction: 348

Materials and methods: 1924

Results: 1606

Discussion: 880

## Abstract

Epilepsy is characterized by unpredictable recurrent seizures resulting from abnormal neuronal excitability. Increasing evidence indicates that aberrant astrocyte signaling to neurons plays an important role in driving the network hyperexcitability, but the underlying mechanism that alters glial signaling in epilepsy remains unknown. Increase in glutamate release by astrocytes participates in the onset and progression of seizures. Epileptic seizures are also accompanied by increase of tumor necrosis factor alpha (TNFα), a cytokine involved in the regulation of astrocyte glutamate release. Here we tested whether TNFα controls abnormal astrocyte glutamate signaling in epilepsy and through which mechanism. Combining $Ca^{2+}$ imaging, optogenetics and electrophysiology, we report that TNFα triggers a $Ca^{2+}$-dependent glutamate release from astrocytes that boosts excitatory synaptic activity in the hippocampus through a mechanism involving autocrine activation of P2Y1 receptors by astrocyte-derived ATP/ADP. In a mouse model of temporal lobe epilepsy such TNFα-driven astrocytic purinergic signaling is permanently active, promotes glial glutamate release and drives abnormal synaptic activity in the hippocampus. Blocking this pathway by inhibiting P2Y1 receptors restores normal excitatory synaptic activity in the inflamed hippocampus. Our findings indicate that targeting the coupling of TNFα with astrocyte purinergic signaling may be a therapeutic strategy for reducing glial glutamate release and normalizing synaptic activity in epilepsy.

**Keywords**: calcium signaling, cytokine, disease, gliotransmission, inflammation, optogenetics

# TOCI

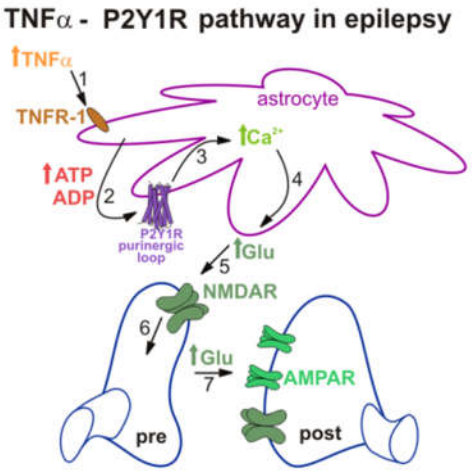


## Main points:

TNFα promotes astrocyte glutamate release via autocrine P2Y1 receptor-mediated signaling.

TNFα-P2Y1 astrocytic pathway drives abnormal synaptic activity in epilepsy and its blocking restores normal hippocampal excitatory synaptic activity.

# Introduction

Epilepsy is one of the most common brain disorders characterized by unpredictable but recurrent seizures originating from an abnormal neuronal excitability. Increase in extracellular glutamate and in excitatory synaptic activity precedes hippocampal epileptiform activity (Chamberlin et al., 1990; During and Spencer, 1993). During seizures extracellular glutamate reaches potentially neurotoxic concentration that could cause neuronal cell death in human hippocampus (During and Spencer, 1993). Therapeutic approaches targeting exclusively neurons have not been completely successful, leading to the suggestion that controlling the signals coming from non-neuronal cells may ameliorate neuronal hyperexcitability (Wetherington et al., 2008; Steinhäuser et al., 2016). Here we focused on astrocytes since enhanced glutamate mediated astrocyte signaling has been implicated in the initiation and sustainment of epileptic activity (Tian et al., 2007; Gómez-Gonzalo et al., 2010; Alvarez-Ferradas et al., 2015). In the healthy brain astrocytes regulate excitatory synaptic activity through glutamate-mediated signaling (Haydon, 2001; Schipke and Kettenmann, 2004; Araque et al., 2014). However, in brain areas involved in the generation and propagation of epileptic activity astrocytes become reactive (Devinsky et al., 2013), this could potentiate glutamate-mediated astrocyte signaling and through an increase of synaptic activity lead to development of seizures (Wetherington et al., 2008; Seifert and Steinhäuser, 2013). How astrocyte glutamate signaling is boosted in epilepsy still remains unknown. Epileptic seizures are accompanied with an increase of proinflammatory cytokines, in particular increase of tumor necrosis factor alpha (TNFα) which correlates with the neuronal cell death (de Bock et al., 1996; Avignone et al., 2008; Patel et al., 2017). TNFα has also been shown to regulate hippocampal synaptic activity by controlling glutamate release from astrocytes (Santello et al., 2011; Habbas et al., 2015). Here, we hypothesized that TNFα induces increased astrocyte glutamate signaling that boosts excitatory synapses in epilepsy. We thus sought to understand the cellular mechanisms by which increased TNFα could act to impair astrocyte signaling to neurons. We found that TNFα increase modulates hippocampal synaptic activity by triggering astrocyte glutamate release via autocrine purinergic signaling and that blocking of this TNFα-purinergic pathway restores normal synaptic activity in an early phase of a mouse model of epilepsy.

## Materials and methods

**Mice.** All experiments were approved by the ethics committee of the University of Paris Descartes (registered numbers CEEA34.EA.027.11 and CEEA16-032) and followed guidelines of the European Union for the care and use of laboratory animals (Council directive 86/609EC). Wild-type and transgenetic male and female C57BL/6 mice were used for experiments. Heterozygous *Cx30-CreERT2* mice (kindly provided by Frank Pfrieger, see (Slezak et al., 2007)) were crossed with homozygous *Ai32* mice (*B6;129S-Gt(ROSA)*$^{26Sortm32(CAG-COP4*H134R/EYFP)Hze}$/J, Jackson Labs) or *Ai95*mice (*B6J; Cg-Gt(ROSA)*$^{26Sortm95.1(CAG-GCaMP6f)Hze}$*/MwarJ*, donated from Hongkui Zeng, Allan Institute)). *CreERT2*–mediated induction of *ChR2* and *GCaMP6f* expression was induced by a single intraperitoneal injection of 1 mg 4-hydroxytamoxifen per approximately 8 g mice weight (Santa Cruz, sc-3542A) around postnatal day 21. At least 2 weeks after tamoxifen injections, mice were sacrificed for experiments.

**Patch-clamp recordings in brain slices.** Coronal hippocampal slices were prepared from 50-60 days-old mice. Whole-cell voltage-clamp and current clamp recordings were obtained from granule cells and molecular layer astrocytes in the dentate gyrus. Animals were anaesthetized with isoflurane, humanely killed by cervical dislocation and decapitated. A 300 μm thick coronal hippocampal slices were cut in an oxygenated (5% $CO_2$ and 95% $O_2$) ice-cold protective NMDG-HEPES extracellular solution containing (in mM): 93 NMDG, 20 HEPES,2.5 KCl, 1.2 $NaH_2PO_4$, 30 $NaHCO_3$, 2 thiourea, 25 D-glucose, 5 sodium ascorbate, 3 sodium pyruvate, 0.5 $CaCl_2$ and 10 $MgCl_2$ (pH 7.3, 310 mOsm). After cutting, slices were transferred to the NMDG-HEPES solution for 7 to 8 min at 34 °C and then incubated at 34°C for 30 min in regular artificial cerebro-spinal fluid (aCSF) containing (in mM): 2.5 KCl, 126 NaCl, 26 $NaHCO_3$, 1.25 $NaH_2PO_4$, 1 sodium pyruvate, 20 mM D-glucose, 2 $CaCl_2$, and 1 $MgCl_2$ (pH 7.4, 310 mOsm). Slices were maintained at room temperature (RT, 22-24°C) for up to 5 hours in the regular oxygenated aCSF before performing electrophysiological recordings or $Ca^{2+}$ imaging experiments. Unless otherwise stated, all salts and chemicals were purchased from Sigma.

Slices were transferred to a recording chamber and perfused with regular aCSF at 3 ml/min speed during the experiments. Whole-cell voltage-clamp recordings were performed on dentate gyrus granule cells with pipettes containing (in mM): 125 $CsMeSO_3$, 10 HEPES, 10 EGTA, 8 TEA-Cl, 5 4-AP, 0.4 GTP-Na, 4 ATP-$Na_2$, 1 $CaCl_2$ and 1 $MgCl_2$ (pH 7.3-7.4, 280-290

mOsm). To perform whole-cell current-clamp recordings from molecular layer astrocytes, we used pipettes (7-8 MΩ) filled with a control intracellular solution containing (in mM): 130 K-Gluconate, 20 HEPES, 10 D-Glucose, 3 ATP-$Na_2$, 1 $MgCl_2$, 0.2 EGTA (pH 7.3-7.4, 280-290 mOsm). The internal solution containing 1,2-bis(2- aminophenoxy)ethane-N,N,N′,N′-tetraacetic acid,Thermo Fisher Scientific (BAPTA) was similar but with the ethylene glycol-bis(2-aminoethylether)-N,N,N′,N′-tetraacetic acid (EGTA) and K-Gluconate replaced with a 40 mM BAPTA. 2'-Deoxy-N6-methyladenosine 3',5'-bisphosphate tetrasodium salt (MRS 2179) and D-2-amino-5-phosphonovalerate (D-AP5) were obtained from Abcam, Apyrase was from Sigma. Axopatch 200B or 700B amplifiers (Molecular Devices) were used for patch-clamp recordings. Signals were sampled at 10 kHz and filtered at 5 kHz or 6 kHz, and analyzed off-line using pClamp 10.4 software (Molecular Devices). Interleaved control slices were kept under the same conditions. Wild-type and wild-type mice injected with tamoxifen were used as controls for optogenetic experiments. Series resistance was monitored every 10 s using 10 mV pulses. For all whole-cell patch-clamp recordings potentials were corrected for a junction potential of -10 mV. Only the recordings in which series and membrane resistance changed less than 20 % were considered for analysis. All experiments were performed at 32-33°C.

mEPSCs were recorded at -70 mV in aCSF containing 0.5 μM Tetrodotoxin cytrate (TTX, Abcam) and 10 μM Gabazine (GBZ, HelloBio). Tumor necrosis factor alpha (TNFα, 10 ng/ml (600 pM), R&D Systems) was pressure applied at the surface of the slices at the level of the molecular layer of dentate gyrus by using a custom made pressure ejection system controlled by electric valves. The pressure was maintained at low level to avoid mechanical movements inside the slices. mEPSCs were detected by setting the event detection threshold at twice the value of standard deviation of the baseline noise. Consecutive 10 s bins of events were analyzed 30 s before, 10 s during and 40 s after the puff application. In experiments using light stimulation, events were counted in 5 s consecutive bins, 15 s before and 20 s during light stimulation. We have used shorter bins for light stimulation experiments since light activation of ChR2 is faster and occurs simultaneously in numerous astrocytes compared to local pressure application of TNFα that reaches its targets slower in the slice. The frequency of mEPSC in ipsilateral and contralateral side was calculated for a period of 60 s (before and after the drug application). For all experimental conditions, only single-peak events were accepted for analysis. For each analyzed bin, frequency and amplitude of mEPSCs was counted for each individual

cell. Data in the presence of pharmacological agents were compared with interleaved control data obtained without the blockers.

**Optical imaging**. *Cx30-CreERT2:GCaMP6f mice*. $Ca^{2+}$ responses during the local puff of TNFα were visualized using a genetically encoded $Ca^{2+}$ indicator *GCaMP6f* expressed in molecular layer astrocytes via a connexin 30 promoter. *GCamP6f* fluorescence was imaged using a 40×water-immersion objective (Olympus) with a custom-built two-photon laser scanning microscope. *GCaMP6f* was excited at 920 nm and emission was detected by external photomultiplier tubes (Hamamatsu). Images were acquired in frame mode (1s per frame) with custom-made software (LabVIEW, National Instruments). Experiments were done in the presence of TTX (0.5 μM) and GBZ (10 μM).

*Cx30-CreERT2:ChR2-EYFPmice*. Molecular layer astrocytes were loaded with the $Ca^{2+}$ indicator Rhod-2 AM (9 μM, Invitrogen) at room temperature (~24 °C) for 1 h with 0.02% Pluronic F-127 (Invitrogen) and 0.6% DMSO (Sigma) in aCSF. During experiments, slices were perfused with aCSF containing TTX (0.5 μM) and GBZ (10 μM). EYFP and the Rhod-2 fluorophore were excited at 850 nm, the two emission fluorescence signals were first separated by a dichroic (560 nm) and the EYFP signal was further filtered through a 525±7 nm bandpass filter (Semrock). Rhod-2 and EYFP emission signals were collected by photomultiplier tubes (Hamamatsu). Single-plane images (500 ms/frame) were acquired at 1Hz using custom-made software. To confirm identity of astrocytes on the basis of EYFP expression, image stacks (1 μM z-spacing, 30-40 optical frames) were acquired after every experiment.

*$Ca^{2+}$ signal analysis*. $Ca^{2+}$ signals were quantified by measuring the pixel intensities of the region of interest (ROI) using custom-made software. Normalized changes in *GCaMP6f* and Rhod-2 fluorescence were expressed as $\Delta F/F = (F - F_0)/F_0$. For experiments with TNFα puff two ROIs were manually set, $ROI_{soma}$ that covers the astrocyte cell body and $ROI_{processes}$ that covers astrocytes processes. ROIs were established according to the morphology of astrocytes determined by *GCaMP6f* expression. To compare the magnitude of $Ca^{2+}$ signals evoked by TNFα puff with the baseline $Ca^{2+}$ signals without biased selection of threshold values, we integrated the consecutive $\Delta F/F_0$ signals as follows: 20 s before (Control), 20 s from the start of TNFα, and the following 20 s (Recovery). Rhod-2 fluorescence was analyzed in the ROI corresponding to the astrocyte cell body and $Ca^{2+}$ responses were defined as light-evoked if the change in F relative to $F_0$ was greater than 2 × s.d. of the baseline signal for at least 3 s. $Ca^{2+}$

signals detected by Rhod-2 were quantified by measuring the area of $\Delta F/F_0$ during the period of light stimulation (10-20 s). The resulting values are expressed as $\Delta F/F0 \cdot s$ in all graphs. Areas of all the $\Delta F/F_0$ signals were determined in Clampfit (Molecular Devices).

**Optogenetic stimulation.** To activate *ChR2* in electrophysiology experiments, full field blue light (470 nm, 10-20s, 0.9-5mW/mm$^2$, Cairn Research, OptoLED) was delivered through the 40×water-immersion objective (Olympus). For $Ca^{2+}$ imaging, 500 ms blue light was delivered at 1 Hz for 10-20 s through the light path of the two-photon microscope and 40× water-immersion objective (Olympus). To avoid saturation of the photomultiper, $Ca^{2+}$ imaging acquisition was performed in between each pulse of the light stimulation, starting 25 ms after the end of the stimulation and stopping 25 ms before the next stimulation.

**Unilateral intracortical kainic acid injection and EEG telemetry.** Stereotaxic injection of kainic acid and placement of telemetric transmitter were performed as described in (Bedner et al., 2015). Prior to the surgery animals were anesthetized by i.p. injection of a mixture of Domitor (1.2mg/kg) and Ketamine (80 mg/kg) and placed in a stereotaxic frame. Surgical incision (2-3 cm) was made through the skin along the dorsal midline from the posterior margin of the eyes to a point midway between scapulae. Using stereotaxic coordinates 1.9 mm posterior to bregma, 1.5 mm from the midline and 1.7 mm from the skull surface, 70 nL of 20 mM kainic acid dissolved in 0.9% NaCl was injected just above the left dorsal hippocampus using a 0.5 µL blunt tip microsyringe (Hamilton, Bonaduz, Switzerland). To limit the reflux after injection, the cannula was left in situ after injection for additional 2 min. Telemetric transmitter (ETA-F10; DataSciences International, St. Paul, USA) was surgically implanted by creating a subcutaneous skin pocket along the animal's dorsal flank using blunt dissection scissors. The biopotential leads of the transmitter were placed on the dura membrane of the brain through cranial perforations (stereotaxic coordinates:1.5 mm from the sagittal suture and 1.9 mm posterior to bregma). Attached leads were then covered with dental cement to ensure electrical isolation, the skin incisions sutured and mouse awaken by i.p. injection of Antisedan (3 mg/kg). After the surgery, for 3 successive days mice were injected with Meloxicam (1 mg/kg s.c.) to reduce the pain. Enrofloxacin (0.25%) was administered via drinking water do reduce the risk of infection. The cage with a mouse was placed on a radio receiving plate (RPC-1; DataSciences International) that sent the captured EEG data to an input exchange matrix and further to the computer running Dataquest A.R.T. 4.00 Gold/Platinum software (DataSciences International).

**Immunohistochemistry.** Wild-type,*Cx30-CreERT2:GCaMP6f* and *Cx30-CreERT2:ChR2-EYFP*mice (P50-60) were anesthetized with sodium pentobarbital (50 mg/kg) and then perfused transcardially with PBS followed by 4% paraformaldehyde (PFA) in 0.15 M phosphate buffer. After fixation overnight in 4% PFA, 50-µm sections were cut using a vibrating microtome. Sections were incubated for 1h in a blocking solution containing 4% normal goat serum (NGS, Sigma Aldrich) and 1% Triton X-100 (Sigma Aldrich) at room temperature. The following primary antibodies were used: chicken anti-GFP (1:500, Invitrogen A10262) mouse anti-glutamine synthetase (1:500, Miilipore MAB302), mouse anti-GFAP (1:500, Sigma G3893), guinea pig anti-NeuN (1:500, Milipore ABN90). After incubation with primary antibodies overnight at 4°C, sections were washed several times and incubated with fluorescently labeled secondary antibodies: goat anti-chicken Alexa 488 (1:250, Invitrogen, A-11039), goat anti-mouse Alexa 555 (1:250, Invitrogen, A11030), goat anti-guinea pig Alexa 633 (1:250, Invitrogen A21105) for 2 or 2.5 h in dark at room temperature. Sections were rinsed and mounted for confocal microscopy (Zeiss LSM-510 or LSM-710).

**Western blot.** Ipsilateral and contralateral hippocampi were dissected out one day post *status epilepticus* and were homogenized in lysis buffer (20 mM HEPES, pH 7.4, 100 mM NaCl, 5 mM EDTA, 1% NP-40, Complete Protease Inhibitor cocktail). Lysates were clarified by centrifugation and protein concentration was determined using a protein assay kit (Biorad). Proteins were separated by reducing 4-12 %, SDS-PAGE, and transferred to a nitrocellulose membrane. The membrane was blocked with 5% non-fat dry milk/0.5% Tween 20 in Tris buffered saline (TBST) for 2h. The membrane was incubated overnight at 4°C with goat anti-TNFα antibody (1:1000, RD System) and mouse anti-tubulin (1:10000, Sigma) in TBST. After three washes in TBST, the membrane was treated with HRP-conjugated secondary antibody for 45 min at room temperature and visualized with an ECL+ detection kit (Amersham). Signals were analyzed using Imagelab software (Biorad).

**Statistics**. Interleaved experiments were performed; no sample size calculation, no randomization or blinding was performed. All tested mice were included in analysis. Data were analyzed and plotted using SigmaPlot and GraphPad Prism. Comparison of two groups of data was carried out using two-tailed paired t-test when samples had Gaussian distributions or Wilcoxon signed rank-test and Man-Whitney test for non-Gaussian distributed data. One-way repeated measures ANOVA (for normal distributed data) or ANOVA on Ranks (for non-normal

distributed data) were used to compare 3 or more groups of data. For time course experiments, the value at time point 0 s was considered as the control value. In cases where ANOVA tests showed significant effects, adequate post hoc comparisons were used to identify significant pairwise differences. $p<0.05$ was considered statistically significant. Some statistical data are showed as box plots (box shoulders indicate 25%-75% intervals, whiskers indicate the 10th and 90th percentiles, "thick line" indicates median value of the data and is showed within the box). Graphs are made with CorelDRAW software. Numbers of cells are given in the parentheses.

# Results

## TNF enhances astrocyte glutamate signaling through $Ca^{2+}$-dependent mechanism

Using acute hippocampal brain slices, increase in TNFα induced by seizures was mimicked by local puff application of the cytokine at a concentration reported to trigger glutamate release from hippocampal astrocytes (600pM; 10 s); (Bezzi et al., 2001)(Habbas et al., 2015). Synaptic activity was monitored by recording miniature excitatory postsynaptic currents (mEPSC) from dentate gyrus granule cells (GC, **Figure 1A**), in the presence of tetrodotoxin (TTX, 0.5 μM) to block action potential firing and of gabazine (10 μM) to block inhibitory $GABA_A$ receptors. TNFα caused an increase in mEPSC frequency of GCs that persisted after the cessation of cytokine application without causing a change of mEPSC amplitude (**Figures 1 A and 1B**). TNFα-induced increase in mEPSCs was completely blocked by D-2-amino-5-phosphonovalerate (D-AP5, 50 μM; Figure **1A**). These observations are in accordance with previous findings demonstrating that TNFα induces a release of glutamate by astrocytes that activates presynaptic NMDA receptors (Habbas et al., 2015). To define the mechanisms required to engage glial response to increased TNFα, we next examined astrocyte $Ca^{2+}$ activity, since glial $Ca^{2+}$ responses have been linked to the synaptic plasticity in the dentate gyrus (Jourdain et al., 2007; Di Castro et al., 2011). $Ca^{2+}$ signals in astrocytes were visualized using *Cx30-CreERT2::GCaMP6* mice in which cytosolic form of *GCaMP6f* is expressed using astrocyte-specific promoter *connexin 30* (*Cx30* (Slezak et al., 2007)). Immunohistochemistry showed *GCaMP6f* to be expressed in cell body and processes of molecular layer astrocytes, whereas *GCaMP6f* expression was not detected in GCs of the dentate gyrus (**Supporting Figure 1**). We found that local increase in

TNFα evoked robust but transient $Ca^{2+}$ rises in astrocyte soma and processes that persisted several seconds after cessation of the cytokine application (**Figures 1C and 1D**). To assess the role of these TNFα-induced $Ca^{2+}$ signals we dialyzed the astrocyte syncytium through a patch pipette containing either a control internal solution containing 0.2 mM ethylene glycol-bis(2-aminoethylether)-N,N,N′,N′-tetraacetic acid (EGTA) or a solution containing 40 mM of the fast $Ca^{2+}$ chelator 1,2-bis(2- aminophenoxy)ethane-N,N,N′,N′-tetraacetic acid (BAPTA). Spread of internal pipette solutions through astrocytes via gap junctions was visualized using the dye Alexa Fluor 594 (25 μM). After 30 min of dialysis, we observed a spread of the dye in the astrocyte syncytium at more than 90 μm from the patched cell (**Figure 1E**). At the same time granule cells were patched with a solution containing Alexa Fluor 488 (25 μM, **Figure 1E**). When astrocytes were dialyzed with the EGTA internal control solution, local rise in TNFα induced an increase of mEPSCs frequency in the GCs (**Figure 1E and 1F**). However, when astrocytes were dialyzed with BAPTA to buffer intracellular $Ca^{2+}$ changes the synaptic effect of TNFα was inhibited (**Figures 1E and 1G**), indicating that the cytokine enhances glutamate release from glial cells through a $Ca^{2+}$-dependent mechanism.

## Astrocyte $Ca^{2+}$ responses to TNFα are mediated by autocrine purinergic signaling

To assess further the mechanism of TNFα action on astrocytes, we next bypassed the cytokine and tried to directly trigger glutamate release from molecular layer astrocytes by optogenetic activation of the light-sensitive channel channelrhodopsin-2 (ChR2). Indeed, we have recently shown that astrocyte photoactivation by ChR2 in CA1 results in a $Ca^{2+}$-dependent glutamate release (Shen et al., 2017). Furthermore, this ChR2-induced glutamate release from CA1 astrocytes, which leads to the activation of neuronal glutamate receptors, requires an autocrine P2Y1 receptor activation (Shen et al., 2017). Therefore, we wanted to examine if the same purinergic loop could be triggered by TNFα in dentate gyrus astrocytes. We used transgenic mice in which ChR2 is expressed under the control of the astrocyte selective promoter *Cx30*. Immunohistochemistry showed that majority of molecular layer astrocytes expressed *ChR2* at the level of soma and their processes, while no *ChR2* expression was detected in the dentate gyrus GCs (**Supporting Figure 2A and 2B**). The cells expressing *ChR2* displayed passive membrane properties typical of astrocytes and could be reliably activated by blue light (**Supporting Figure**

**2C**). To monitor $Ca^{2+}$ signals, we loaded astrocytes of *Cx30-CreERT2::ChR2-EYFP* mice with membrane-permeant form of the red $Ca^{2+}$ fluorescent indicator Rhod-2 (**Figure 2A**). This loading method restricts monitoring of $Ca^{2+}$ signals in the astrocyte cell body only. Light-induced astrocyte activation triggered somatic $Ca^{2+}$ elevations in *EYFP*-expressing astrocytes with mean amplitude of 225.6 ± 21.54 F/F that peaked 5.6 ± 0.3 s after the onset of the stimulation (24 cells, 5 animals). Similar to CA1 (Shen et al., 2017), light-triggered $Ca^{2+}$ signals in astrocyte cell body in dentate gyrus were dependent on P2Y1 receptor activation, since 2'-Deoxy-N6-methyladenosine 3',5'-bisphosphate tetrasodium salt (MRS 2179, 10 μM) reduced these responses (**Figure 2A**). Light-evoked $Ca^{2+}$ signals could not be suppressed completely by MRS 2179. Although $Ca^{2+}$ permeability of *ChR2* is low (Nagel et al., 2003), these residual $Ca^{2+}$ response remaining after P2Y1 receptors block could represent the sole contribution of the optogenetic actuator or its amplification by $Ca^{2+}$-induced $Ca^{2+}$ release. TNFα-induced $Ca^{2+}$ signals in astrocytes were also dependent on P2Y1 receptor activation. Remarkably, blocking these purinergic receptors with MRS 2179 completely abolished glial $Ca^{2+}$ responses induced by TNFα (**Figure 2B**), suggesting that P2Y1-dependent loop play a key role in activation of astrocytes by TNFα.

## TNFα boosts astrocyte glutamate release through glial autocrine purinergic signaling

If activation of the purinergic loop controls glutamate release from astrocytes upon TNFα increase, then blocking P2Y1 receptors should be able to inhibit glutamate release and prevent the change of excitatory synaptic activity induced by the cytokine. We first selectively increased astrocyte glutamate release by ChR2 stimulation and monitored excitatory synaptic activity of GCs. We found that activation of molecular layer astrocytes by shining light for 20 s, increased the frequency of mEPSC without changing their amplitude, suggesting a facilitating action at the level of presynaptic terminals (**Figure 3A-3C**). The modulation of synaptic transmission induced by light activation of astrocytes was inhibited by D-AP5 (**Figure 3A and 3B**), suggesting that observed synaptic facilitation relies on astrocyte glutamate release activating presynaptic NMDA receptors, as this is the case for TNFα (**see Figure 1A and 1B**). As a control experiment, we verified that similar light stimulation did not induce a change in the frequency of granule cells

mEPSCs in wild-type mouse (**Supporting Figure 3**). Consistent with the block of the cytokine- and light-triggered $Ca^{2+}$ responses in astrocytes by MRS 2179, the block of P2Y1 receptors also prevented the increase of mEPSC frequency induced by light and by TNFα (**Figure 3D**). Blocking P2Y1 receptors had larger effects on the increase of mEPSC frequency than on the $Ca^{2+}$ responses induced by astrocyte photoactivation (**see Figure 2A**), indicating that the P2Y1 receptor-dependent $Ca^{2+}$ responses are sufficient for astrocyte-mediated synaptic enhancement. P2Y1 receptors are activated by extracellular ATP/ADP and we reasoned that if activation of P2Y1 receptors mediates astrocyte glutamate release, a decrease in the extracellular ATP/ADP concentration should in contrast reduce P2Y1 receptor activation (Vigne et al., 1998) and thereby abrogate astrocyte glutamate signaling. We therefore tested the effect of light and TNFα in the presence of apyrase, an enzyme with ATP/ADPase activity, to decrease the extracellular level of purines. We have used a low dose of 25 U/mL apyrase to minimize enzyme actions related to potassium and independent of purines (Madry et al., 2018). We found that apyrase treatment resulted in a complete block of light- and TNFα-induced increase in synaptic activity (**Figure 3E**), indicating that TNFα boosts glutamate signaling via astrocytic autocrine purinergic signaling.

## Blocking TNFα-activated purinergic signaling in astrocytes restores normal glutamatergic activity in epilepsy

Could activation of astrocyte purinergic signaling by TNFα be responsible for the increased glutamatergic synaptic activity in epilepsy? To answer this question, we used an animal model of temporal lobe epilepsy (TLE) (Bedner et al., 2015). In this TLE model unilateral intracortical kainate injection triggers *status epilepticus* characterized by the typical EEG signature (**Figure 4A**), followed by a silent period of 4-5 days (latent period) and the occurrence of spontaneous recurrent seizures (chronic period) (see Bedner et al., 2015). The latent period is thought to involve changes that act to transform the normal neuronal network into a hyperexcitable one (Goldberg and Coulter, 2014). Moreover, compromised dentate gyrus function during the latent period of TLE has been proposed to promote development of seizures (Pathak et al., 2007). Thus, we examined astrocyte glutamate signaling at the end of this latent period. First, we verified that the level of TNFα was higher in the ipsilateral hippocampus than in the contralateral

hippocampus after *status epilepticus* (**Supporting Figure 4**). We found that astrocytes in the molecular layer of the ipsilateral dentate gyrus had a higher GFAP immunoreactivity, larger soma and thicker primary processes compared with astrocytes in the contralateral side at 4 days post kainate injection (**Figure 4B**). This morphological inspection indicates that astrocytes are reactive in the ipsilateral dentate gyrus. Next, we found that TNFα evoked an increase of the mEPSC frequency in the contralateral side, but that the cytokine had no effect in the ipsilateral side 4 days post kainate injection (**Figure 4C**). These findings suggest that the cytokine-triggered signaling pathway could be already activated in the ipsilateral side, occluding the effect of exogenously applied TNFα. Accordingly, excitatory synaptic activity of GCs was higher in the ipsilateral than in the contralateral side (**Figure 4D, 4E**). Notably, no difference in the mEPSC amplitude was detected between ipsi- and contralateral side (**Figure 4F**), indicating that upregulation of synaptic activity in the kainate injected side depends on presynaptic mechanisms, as was the case for responses induced by TNFα or by the direct light activation of astrocytes. Next we investigated if simply blocking glial purinergic signaling could restore normal synaptic activity in GCs. Indeed, blocking P2Y1 receptors decreased mEPSC frequency in the ipsilateral side but not in the contralateral side (**Figure 4D and 4E**). Remarkably, this inhibition of synaptic activity in the ipsilateral side by MRS 2179 restored mEPSC frequency to the value that we measured in the contralateral side (**Figure 4E**). These results demonstrate that blocking of TNFα-P2Y1 pathway normalizes glutamate release from astrocytes during the latent period of TLE.

## Discussion

Astrocyte signaling plays a crucial role in controlling neuronal activity, both physiologically and in disease. In epilepsy, increased astrocyte glutamate signaling contributes to the excessive neuronal activity, maintenance and spread of seizure activity (Tian et al., 2007). Consequently, characterizing the signaling mechanisms that control excessive glutamate signaling by astrocytes is important for understanding the transition to abnormal neuronal activity. In the present study we have characterized the mechanisms through which TNFα promotes the increase in astrocyte glutamate release (Habbas et al., 2015) and our data suggest that this signaling pathway is constitutively active at the end of the latent phase in a mouse model of TLE. Specifically, we

show that the cytokine is able to boost glutamate release from astrocytes through a mechanism involving astrocyte $Ca^{2+}$ signaling and purinergic P2Y1 receptor activation.

Interactions between TNFα and P2Y1 receptor-mediated signaling in controlling astrocyte glutamate release had been previously investigated, however, no consensus emerged from these studies (Bezzi et al., 2001; Domercq et al., 2006; Santello et al., 2011; Pascual et al., 2012), and it remained unclear whether the cytokine positively modulates P2Y1 receptor-mediated $Ca^{2+}$ response of astrocytes or promotes the docking of glutamate vesicles in these cells. We show here that increased TNFα exert complete control over P2Y1 receptor-mediated signaling in dentate gyrus astrocytes. Indeed, increased $Ca^{2+}$ signaling and glutamate release of astrocytes induced by TNFα were entirely blocked by an antagonist of P2Y1 receptors. Our data also indicate that P2Y1 receptors are activated through an autocrine mechanism involving ATP release by astrocytes since astrocyte-mediated increase in excitatory synaptic activity induced either by selective optogenetic activation or by TNFα was blocked by the ATP-degrading apyrase.

We cannot totally exclude that TNFα-triggered purinergic signaling in astrocytes is mediated through the recruitment of microglial cells. Indeed, these cells also express receptors (Zhang et al., 2014) and the activation of these receptors could induce the release of microglial mediators that would recruit astrocyte signaling. In particular, microglial ATP was shown to modulate CA1 excitatory synapses through P2Y1 receptor-mediated control of astrocyte glutamate release (Pascual et al., 2012). However, Habbas et al., 2015 previously showed that inducing the expression of the TNFα receptor TNFR1a specifically in astrocytes of TNFR1 knockout mice was sufficient to restore the effect TNFα on mEPSC frequency in DG granule cells.

P2Y1 receptors are expressed by astrocytes but also by inhibitory interneurons in the hippocampus (Bowser, 2004; Jourdain et al., 2007; Pascual et al., 2012; Tan et al., 2017). TNFα-triggered P2Y1 receptor-dependent $Ca^{2+}$ signaling of DG astrocytes is unlikely to be secondary to increased activity of hippocampal interneurons since we have performed experiments in conditions that minimized the influence of neuronal network activity and prevent the activation of $GABA_A$ receptors, indicating that interneurons are not involved in the effects of TNFα on excitatory synaptic activity in DG. This does not exclude the possibility that the cytokine has some effects on inhibition (e.g. Stellwagen et al., 2005). In the case of epilepsy disruption of

inhibitory transmission in GCs has also been shown to enhance excitability of these cells during the latent period (Pathak et al., 2007). Finally, our observation that specific activation of astrocytes by optogenetics mimics the effects of TNFα on the frequency of mEPSCs and also involves P2Y1 receptor activation and the presence of extracellular ATP further supports the idea that purinergic signaling in astrocytes, and not in other cell types (e.g. oligodendrocytes, references in Rivera, Vanzulli Butt Current Drug Targets 2016), is the key element mediating the effects of TNFα on excitatory synaptic activity in GCs.

Previous reports showed that modulation of astrocyte signaling may have an important and perhaps causal role for neuronal dysfunction and could represent a therapeutical target for diseases such as epilepsy (Ding et al., 2007; Tian et al., 2007; Gómez-Gonzalo et al., 2010; Bedner et al., 2015), multiple sclerosis (Habbas et al., 2015) or ischemia (Beppu et al., 2014). Moreover, specific activation of astrocyte P2Y1 receptors was shown to be associated with inflammation (Franke et al., 2012), cerebral ischemia (Kuboyama et al., 2011) or Alzheimer disease (Delekate et al., 2014), leading to the view that controlling the activity of these receptors ameliorates inflammation and brain damage. Our data indicate that blocking the autocrine P2Y1 pathway activated by TNFα normalized synaptic activity in a mouse model of TLE, which reproduces many features of the human disease, including astrogliosis (Bedner et al., 2015). Increased TNFα level has been associated with seizure generation in epilepsy (de Bock et al., 1996; Avignone et al., 2008; Patel et al., 2017). Our results thus strongly suggest that the increased level of the cytokine in an early period of TLE is responsible for the increased excitatory synaptic transmission in GCs since the synaptic effect of TNFα was occluded in the ipsilateral and not in the contralateral hippocampus. Astrogliosis as seen with GFAP staining was most evident in the ipsilateral hippocampus (see also (Bedner et al., 2015) and this correlated with the occlusion of the synaptic effect of TNFα, modifications of synaptic activity and permanent activation of the purinergic loop in the latent TLE period. This is in full agreement with the idea that reactive astrocytes in different pathological conditions are characterized by an increased P2Y1 receptor signaling (Kuboyama et al., 2011; Delekate et al., 2014). Functional interactions between cytokines and the gliotransmitters glutamate and ATP are thought to contribute in promoting epileptic seizures (Vezzani et al., 2008a; b; Rassendren and Audinat, 2016). This does not exclude, however, that other cell types and pathways are involved or regulate this canonical signaling. Microglial cells are known to be essential for the production of

TNFα in pathological conditions (Olmos and Lladó, 2014). Microglia-controlled TNFα-mediated signaling has been proposed to promote formation of neurotoxic and reactive astrocytes in different brain diseases (Liddelow et al., 2017) and to favor glutamate release from astrocytes, which could lead to neurotoxicity (Bezzi et al., 2001).

Application of our findings in designing a therapeutic approach requires caution since TLE is the most common drug-resistant type of epilepsy. Understanding the progression of epileptogenesis during the latent period may be crucial to ensure the early diagnosis and management of this condition, and the coupling between TNFα and astrocytic P2Y1 receptors may hold potential as a useful biomarker. Indeed, our data do show that blocking of the TNFα-driven increase in astrocyte glutamate release can prevent and normalize excitatory synaptic activity in a mouse model of TLE during this latent period. Further research directed at identifying the precise mechanism by which TNFα engages P2Y1 receptors in epilepsy could provide a framework within which targeted therapeutic intervention could become effective.

## References


Alvarez-Ferradas C, Morales J.C., Wellmann M, Nualart F, Roncagliolo M, Fuenzalida M, Bonansco C. (2015). Enhanced astroglial $Ca^{2+}$ signaling increases excitatory synaptic strength in the epileptic brain. Glia *63*, 1507– 1521. doi: 10.1002/glia.22817.

Araque A, Carmignoto G, Haydon P.G., Oliet S.H.R., Robitaille R, Volterra A. (2014). Gliotransmitters Travel in Time and Space. Neuron *81*, 728– 739. doi: 10.1016/j.neuron.2014.02.007.

Avignone E, Ulmann L, Levavasseur F, Rassendren F, Audinat E. (2008). Status epilepticus induces a particular microglial activation state characterized by enhanced purinergic signaling. Journal of Neuroscience *28,* 9133– 9144. doi: 10.1523/JNEUROSCI.1820-08.2008.

Bedner P, Dupper A, Hüttmann K, Müller J, Herde M.K., Dublin P, Deshpande T, Schramm J, Häussler U, Haas C.A., Henneberger C, Theis M, Steinhäuser C. (2015). Astrocyte uncoupling as a cause of human temporal lobe epilepsy. Brain *138,* 1208– 1222. doi: 10.1093/brain/awv067.

Beppu K, Sasaki T, Tanaka K.F., Yamanaka A, Fukazawa Y, Shigemoto R, Matsui K. (2014). Optogenetic countering of glial acidosis suppresses glial glutamate release and ischemic brain damage. Neuron *81,* 314– 320. doi: 10.1016/j.neuron.2013.11.011.

Bezzi P, Domercq M, Brambilla L, Galli R, Schols D, De Clercq E, Vescovi A Bagetta G, Kollias G, Meldolesi J, Volterra A. (2001). CXCR4-activated astrocyte glutamate release via

TNFalpha: amplification by microglia triggers neurotoxicity. Nature Neuroscience *4,* 702– 710. doi:10.1038/89490.

de Bock F, Dornand J, Rondouin G. (1996). Release of TNF alpha in the rat hippocampus following epileptic seizures and excitotoxic neuronal damage. Neuroreport *7,* 1125– 1129.

Bowser D.N., & Khakh B.S. (2004). ATP Excites Interneurons and Astrocytes to Increase Synaptic Inhibition in Neuronal Networks. Journal of neuroscience *24*, 8606– 8620. doi: 10.1523/JNEUROSCI.2660-04.2004.

Di Castro M.A., Chuquet J, Liaudet N, Bhaukaurally K, Santello M, Bouvier D, Tiret P, Volterra A. (2011). Local $Ca^{2+}$ detection and modulation of synaptic release by astrocytes. Nature Neuroscience *14,* 1276– 1284. doi: 10.1038/nn.2929.

Chamberlin N.L., Traub R.D., Dingledine R. (1990). Role of EPSPs in initiation of spontaneous synchronized burst firing in rat hippocampal neurons bathed in high potassium. Journal of Neurophysiology *64,* 1000–1008. doi:10.1152/jn.1990.64.3.1000.

Delekate A, Füchtemeier M, Schumacher T, Ulbrich C, Foddis M, Petzold G.C. (2014). Metabotropic P2Y1 receptor signalling mediates astrocytic hyperactivity in vivo in an Alzheimer's disease mouse model. Nature Communications *5,* 5422. doi: 10.1038/ncomms6422.

Devinsky O, Vezzani A, Najjar S, De Lanerolle N.C., Rogawski M.A. (2013). Glia and epilepsy: excitability and inflammation. Trends in Neurosciences *36,* 174– 184. doi: 10.1016/j.tins.2012.11.008.

Ding S, Fellin T, Zhu Y, Lee S-Y, Auberson Y.P., Meaney D.F., Coulter D.A., Carmignoto G, Haydon P.G. (2007). Enhanced astrocytic $Ca^{2+}$ signals contribute to neuronal excitotoxicity after status epilepticus. Journal of Neuroscience [Internet] 27:10674– 10684. Available from: http://www.jneurosci.org/cgi/doi/10.1523/JNEUROSCI.2001-07.2007.

Domercq M, Brambilla L, Pilati E, Marchaland J, Volterra A, Bezzi P. (2006). P2Y1 receptor-evoked glutamate exocytosis from astrocytes: Control by tumor necrosis factor-alpha and prostaglandins. Journal of Biological Chemistry *281*, 30684– 30696. doi:10.1074/jbc.M606429200.

During M.J., Spencer D.D. (1993). Extracellular hippocampal glutamate and spontaneous seizure in the conscious human brain. Lancet *341*, 1607– 1610.

Franke H, Verkhratsky A, Burnstock G, Illes P. (2012). Pathophysiology of astroglial purinergic signalling. Purinergic Signalling *8,* 629– 657. doi: 10.1007/s11302-012-9300-0.

Goldberg E.M., Coulter D.A. (2014). Mechanisms of epileptogenesis: a convergence on neural circuit dysfunction. Nature Reviews Neuroscience *14*, 337– 349. doi:10.1038/nrn3482.

Gómez-Gonzalo M, Losi G, Chiavegato A, Zonta M, Cammarota M, Brondi M, Vetri F, Uva L, Pozzan T, de Curtis M, Ratto G.M., Carmignoto G. (2010). An excitatory loop with astrocytes contributes to drive neurons to seizure threshold. PLoS Biology *8,* e1000352. doi: 10.1371/journal.pbio.1000352.

Habbas S, Santello M, Becker D, Stubbe H, Zappia G, Liaudet N, Klaus F.R., Kollias G, Fontana A, Pryce C.R., Suter T, Volterra A. (2015). Neuroinflammatory TNFα Impairs Memory via Astrocyte Signaling. Cell *163,* 1730– 1741. doi: 10.1016/j.cell.2015.11.023.

Haydon P.G. (2001). GLIA: listening and talking to the synapse. Nature Reviews Neuroscience *2,* 185– 193. doi:10.1038/35058528.

Jourdain P, Bergersen L.H., Bhaukaurally K, Bezzi P, Santello M, Domercq M, Matute C, Tonello F, Gundersen V, Volterra A. (2007). Glutamate exocytosis from astrocytes controls synaptic strength. Nature Neuroscience *10,* 331– 339. doi: 10.1038/nn1849.

Kuboyama K, Harada H, Tozaki-Saitoh H, Tsuda M, Ushijima K, Inoue K. (2011). Astrocytic P2Y(1) receptor is involved in the regulation of cytokine/chemokine transcription and cerebral damage in a rat model of cerebral ischemia. Journal of Cerebral Blood Flow & Metabolism *31,* 1930–1941. doi: 10.1038/jcbfm.2011.49.

Liddelow S.A., Guttenplan K.A., Clarke L.E., Bennett F.C., Bohlen C.J., Schirmer L, Bennett M.L., Münch A.E., Chung W-S, Peterson T.C., Wilton D.K., Frouin A, Napier B.A., Panicker N, Kumar M, Buckwalter M.S., Rowitch D.H., Dawson V.L., Dawson T.M., Stevens B, Barres B.A. (2017). Neurotoxic reactive astrocytes are induced by activated microglia. Nature *541,* 481-487. doi: 10.1038/nature21029.

Madry C, Arancibia-Cárcamo I.L., Kyrargyri V, Chan V.T.T., Hamilton N.B., Attwell D. (2018). Effects of the ecto-ATPase apyrase on microglial ramification and surveillance reflect cell depolarization, not ATP depletion. Proceedings of the National Academy of Sciences of the United States of America *13,* E1608- E1617. doi: 10.1073/pnas.1715354115.

Nagel G, Szellas T, Huhn W, Kateriya S, Adeishvili N, Berthold P, Ollig D, Hegemann P, Bamberg E. (2003). Channelrhodopsin-2, a directly light-gated cation-selective membrane channel. Proceedings of the National Academy of Sciences of the United States of America *100,* 13940– 13945. doi: 10.1073/pnas.1936192100.

Olmos G, Lladó J. (2014). Tumor necrosis factor alpha: A link between neuroinflammation and excitotoxicity. Mediators Inflammation *2014,* 861231. doi: 10.1155/2014/861231.

Pascual O, Ben Achour S, Rostaing P, Triller A, Bessis A. (2012). Microglia activation triggers astrocyte-mediated modulation of excitatory neurotransmission. Proceedings of the National Academy of Sciences of the United States of America *109,* E197– E205. doi: 10.1073/pnas.1111098109.

592 Patel D.C., Wallis G, Dahle E.J., McElroy P.B., Thomson K.E., Tesi R.J., Szymkowski D.E.,
593 West P.J., Smeal R.M., Patel M, Fujinami R.S., White H.S., Wilcox K.S. (2017). Hippocampal
594 TNFα Signaling Contributes to Seizure Generation in an Infection-Induced Mouse Model of
595 Limbic Epilepsy. eNeuro *4,* pii: ENEURO.0105-17.2017. doi: 10.1523/ENEURO.0105-17.2017.

596 Pathak H.R., Weissinger F, Terunuma M, Carlson G.C., Hsu F-C, Moss S.J., Coulter D.A.
597 (2007). Disrupted Dentate Granule Cell Chloride Regulation Enhances Synaptic Excitability
598 during Development of Temporal Lobe Epilepsy. Journal of Neuroscience *27,* 14012– 14022.
599 doi: 10.1523/JNEUROSCI.4390-07.2007.

600 Rassendren F, Audinat E. (2016). Purinergic signaling in epilepsy. Journal of Neuroscience
601 Research *94,* 781– 793. doi: 10.1002/jnr.23770.

602 Rivera A, Vanzulli I, Butt A.M., (2016). A Central Role for ATP Signalling in Glial Interactions
603 in the CNS. Current Drug Targets. *17,* 1829– 1833.
604
605 Santello M, Bezzi P, Volterra A. (2011). TNFα Controls Glutamatergic Gliotransmission in the
606 Hippocampal Dentate Gyrus. Neuron *69,* 988– 1001. doi: 10.1016/j.neuron.2011.02.003.

607 Schipke C.G. & Kettenmann H. (2004). Astrocyte responses to neuronal activity. Glia *47,* 226–
608 232. doi: 10.1002/glia.20029.

609 Seifert G. & Steinhäuser C. (2013). Neuron–astrocyte signaling and epilepsy. Experimental
610 Neurology *244,* 4– 10. doi: 10.1016/j.expneurol.2011.08.024.

611 Shen W, Nikolic L, Meunier C, Pfrieger F, Audinat E. (2017). An autocrine purinergic signaling
612 controls astrocyte-induced neuronal excitation. Scientific Reports *7,* 11280. doi:
613 10.1038/s41598-017-11793-x.

614 Slezak M, Goritz C, Niemiec A, Frisen J, Chambon P, Metzger D, Pfrieger F.W. (2007).
615 Transgenic mice for conditional gene manipulation in astroglial cells. Glia *55,* 1565– 1576. doi:
616 10.1002/glia.20570.

617 Steinhäuser C, Grunnet M, Carmignoto G. (2016). Crucial role of astrocytes in temporal lobe
618 epilepsy. Neuroscience *323,* 157– 169. doi: 10.1016/j.neuroscience.2014.12.047.

619 Tan Z, Liu Y, Xi W, Lou H, Zhu L, Guo Z, Mei L, Duan S. (2017). Glia-derived ATP inversely
620 regulates excitability of pyramidal and CCK-positive neurons. Nature Communications *8,*
621 13772. doi: 10.1038/ncomms13772.

622 Tian G.F., Azmi H, Takano T, Xu Q, Peng W, Lin J, Oberheim N, Lou N, Wang X, Zielke H.R.,
623 Kang J, Nedergaard M. (2005). An astrocytic basis of epilepsy. Nature Medicine *11,* 973- 981.
624 doi: 10.1038/nm1277.

Vezzani A, Balosso S, Ravizza T. (2008a). The role of cytokines in the pathophysiology of epilepsy. Brain, Behavior, and Immunity *22,* 797– 803. doi: 10.1016/j.bbi.2008.03.009.

Vezzani A, Ravizza T, Balosso S, Aronica E. (2008b). Glia as a source of cytokines: Implications for neuronal excitability and survival. Epilepsia *49,* 24– 32. doi: 10.1111/j.1528-1167.2008.01490.x.

Vigne P, Breittmayer J.P., Frelin C. (1998). Analysis of the influence of nucleotidases on the apparent activity of exogenous ATP and ADP at P2Y1 receptors. British Journal of Pharmacology *125,* 675– 80. doi: 10.1038/sj.bjp.0702115.

Wetherington J, Serrano G, Dingledine R. (2008). Astrocytes in the Epileptic Brain. Neuron *58,* 168– 178. doi: 10.1016/j.neuron.2008.04.002.

Zhang Y, Chen K, Sloan S.A., Bennett M.L., Scholze A.R., O'Keeffe S, Phatnani H.P., Guarnieri P, Caneda C, Ruderisch N, Deng S, Liddelow S.A., Zhang C, Daneman R, Maniatis T, Barres B.A., Wu J.Q. (2014). An RNA-Sequencing Transcriptome and Splicing Database of Glia, Neurons, and Vascular Cells of the Cerebral Cortex. Journal of Neuroscience *34,* 11929–11947. doi:10.1523/JNEUROSCI.1860-14.2014.

## Data availability statement

The data that support the findings of this study are available from the corresponding author upon reasonable request.

## Figure legends

**Figure 1.**

**TNF enhances astrocyte glutamate signaling through Ca2+-dependent mechanism. (A)** Schematic of TNFα puff application (600 pM, 10 s) onto molecular layer astrocytes while recording synaptic activity from patch-clamped granule cell of the dentate gyrus (DG). Representative traces show the frequency of mEPSCs before and after application of TNFα in control conditions and with the NMDA receptor antagonist D-AP5 (50 μM) in the presence of TTX (0.5 μM) and gabazine (10 μM). **(B)** Time course of the mean effect of TNFα. TNFα significantly increased the mEPSC frequency in the control conditions but the cytokine effect is attenuated in the presence of D-AP5 (for control: n=8 cells, 3 animals, *p<0.05;for D-AP5: n=9,

4 animals, p=0.47; One-way RM ANOVA on Ranks, Dunn's post hoc test,). TNFα did not induce a change in the amplitude of mEPSCs (n=8 cells, 3 animals, p=0.844; One-way RM ANOVA on Ranks). Inset: aligned mEPSC events (10-15 events, in grey) and their average value (in black) before and after TNFα puff application. **(C)** Time projections of GCaMP6f fluorescence of Cx30-CreERT2:GCaMP6f mice taken at 1 Hz, 20 s before and 20 s from the onset of the TNFα puff application to the surface of molecular layer. Dotted lines indicate ROIs covering astrocyte soma (ROIsoma) and process territory (ROIprocesses). Images and examples of traces obtained from astrocyte soma and processes show that TNFα evokes astrocyte Ca2+ responses. **(D)** Box plots of average responses from astrocyte somata and processes show significant increase in Ca2+ responses evoked by TNFα in control conditions (n=11, 2 animals, One-way RM ANOVA, Bonferroni post hoc; *p<0.05, **p<0.01). **(E)** Astrocyte network in molecular layer labeled with Alexa Fluor 594 (magenta) during whole-cell patch-clamp recording from a single astrocyte. An adjacent granule cell is patched with a pipette containing Alexa Fluor 488 (cyan). Example traces and mean data **(F, G)** demonstrating that TNFα evoked increase in mEPSC frequency is maintained when the astrocyte network is dialyzed with a control EGTA internal solution but abolished when the glial network is dialyzed with BAPTA (EGTA internal: n=9, 3 animals, *p<0.05, **p<0.01; BAPTA internal: n=6, 3 animals, p=0.61; One-way RM ANOVA, Bonferroni Post hoc). Data are presented as mean ± SEM for time course experiments. Orange bars indicate TNFα puff applications in all figures. See also Supporting Figure 1.

**Figure 2.**

**Autocrine purinergic signaling mediates astrocyte $Ca^{2+}$ responses to TNFα. (A)** Two-photon images obtained from Cx30-CreERT2:ChR2-EYFP mice show Rhod-2 loaded molecular layer astrocyte expressing ChR2-EYFP. Traces illustrate changes in Rhod-2 emission intensity ( F/F) of a ChR2-EYFP positive astrocyte in response to photostimulation in control conditions and during bath application of the purinergic P2Y1R antagonist MRS 2179 (10 μM). Dotted line represents baseline level of $Ca^{2+}$ signals. Summary box plots show the inhibitory effect of MRS 2179 on $Ca^{2+}$ responses evoked by light in astrocytes (n=12, 5 animals, Wilcoxon signed-rank test, ***p<0.001). Blue bars indicate light stimulation in all the figures. **(B)** Time projections of GCaMP6f fluorescence of Cx30-CreERT2:GCaMP6f mice taken at 1 Hz, 20 s before and 20 s

687 from the onset of the TNFα puff application to the surface of molecular layer area of dentate
688 gyrus in the presence of MRS 2179. Examples of traces and box plots show that TNFα evoked
689 $Ca^{2+}$ excitation of astrocytes is attenuated when P2Y1 receptors are blocked by MRS 2179
690 (n=11, 2 animals, for ROIsoma: p=0.07, for ROIprocesses: p=0.148; One-way RM ANOVA on
691 Ranks). See also Supporting Figure 2.
692
693 **Figure 3.**
694 **TNFα boosts astrocyte glutamate release through glial autocrine purinergic signaling. (A)**
695 Schematic of light stimulation experiments; a granule cell was whole-cell recorded while
696 molecular layer astrocytes were activated by blue light. Examples of traces show granule cell
697 mEPSCs before and during light stimulation in control conditions and in the presence of 50 μM
698 D-AP5. **(B)** Summary graphs showing that D-AP5 blocks the increase of mEPSC frequency
699 induced by light activation of astrocytes (Control: n=9, 4 animals, *p<0.05, **p<0.01; D-AP5:
700 n=11, 4 animals, p=0.31; One-way RM ANOVA on Ranks, Dunn's post hoc). **(C)** Control
701 mEPSC amplitude remains unchanged during light activation of astrocytes (n=9, 4 animals,
702 p=0.23; One-way RM ANOVA). Inset: aligned mEPSC events (10-15 events, in grey) and their
703 average value (in black) before and after light activation of astrocytes. **(D)** Blocking P2Y1
704 receptors with 10 μM MRS 2179 prevents astrocyte-dependent increase in mEPSC frequency
705 induced by light stimulation or by TNFα (light stimulation: ControlM: n=9, 4 animals, MRS
706 2179: n=12, 4 animals, p=0.293; TNFα: ControlM:n=12, 4 animals; MRS 2179: n=9, 4 animals;
707 p=0.302; *p<0.05, **p<0.01; One-way RM ANOVA on RanksDunn's post hoc); **(E)** Degrading
708 extracellular ATP/ADP by apyrase (25 U/mL) blocks astrocyte-mediated increase of mEPSC
709 frequency induced by light stimulation or by TNFα (light stimulation: ControlA: n=9, 3 animals;
710 Apyrase: n=7, 3 animals, p=0.1; TNFα: ControlA: n=9, 3 animals, Apyrase: n=8, 3 animals,
711 p=0.691;*p<0.05, **p<0.01; One-way RM ANOVA on Ranks, Dunn's post hoc). Data are
712 presented as mean ± SEM. See also Supporting Figure 3.
713
714 **Figure 4.**
715 **Blocking TNFα-activated purinergic signaling in astrocytes restores normal glutamatergic**
716 **activity in epilepsy. (A)** Schematic drawing illustrating unilateral stereotactic injection of kainic
717 acid into the neocortex just above the dorsal hippocampus of a wild-type mouse that was then

monitored by video and cortical EEG telemetric recordings. An example of EEG recording illustrates bursts of spike discharges during status epilepticus. **(B)** Confocal images of GFAP and NeuN immunostaining in the ipsilateral and contralateral dentate gyrus of a wild-type mouse 4 days after kainate injection. Note the stronger GFAP immunoreactivity, the larger somata and thicker proximal processes of astrocytes in ipsilateral side. **(C)** Application of 600 pM TNFα did not further increase mEPSC frequency in the ipsilateral side 4days after kainate injection, suggesting that the cytokine-triggered signaling pathway is already activated (n=6, 3 animals, p=0.66; One-way RM ANOVA). Application of TNFα could still induce an increase in the mEPSC frequency in contralateral side (One-way RM ANOVA, Bonferroni post-hoc, *p<0.05, **p<0.01). **(D, E)** Examples of traces and boxed plots obtained from granule cells 4 days after kainate injection showing that blocking P2Y1 receptors decreased mESPC frequency in the ipsilateral side but not in the contralateral side (for ipsilateral side: n=8, 3 animals, **p<0.01; for contralateral side: n=7, p=0.93; Wilcoxon Signed-rank test). Note that baseline mEPSC frequency is higher in ipsilateral side compared with contralateral side (Man-Whitney test; **p<0.01). Block of P2Y1 receptors in ipsilateral side restores the normal mEPSC frequency measured in contralateral side (p=0.152, Man-Whitney test). **(F)** Boxed plots obtained from dentate gyrus granule cells 4 days after kainate injection showing that mEPSC amplitude is not changed in the ipsilateral compared with contralateral side (p=0.463, Mann-Whitney test). Data are presented as mean ± SEM for time course experiments.

Figure 1

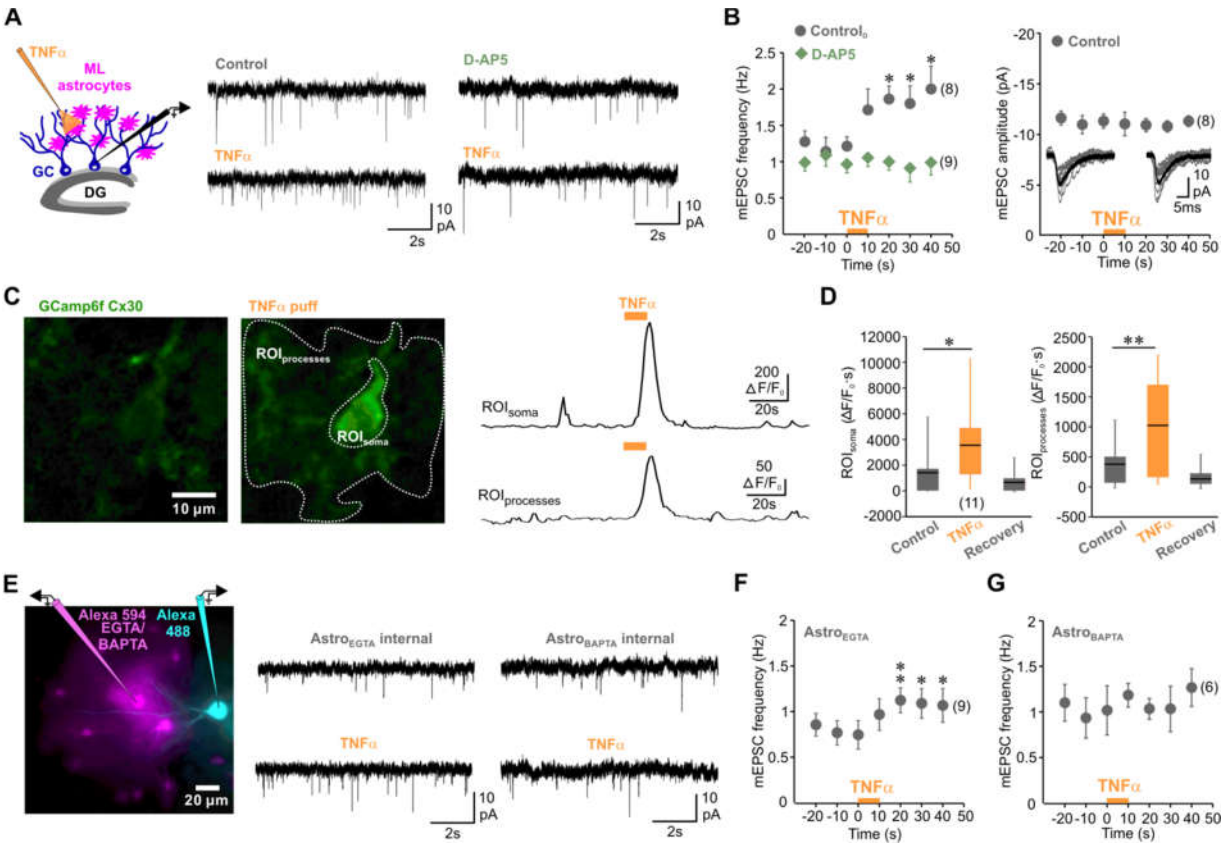
A
TNFα
ML
astrocytes
GC
DG
Control
D-AP5
TNFα
TNFα
10 pA
2s
10 pA
2s
B
Control
D-AP5
mEPSC frequency (Hz)
(8)
(9)
TNFα
Time (s)
Control
mEPSC amplitude (pA)
(8)
10 pA
5ms
TNFα
Time (s)
C
GCamp6f Cx30
TNFα puff
ROIprocesses
ROIsoma
10 μm
TNFα
ROIsoma
200 ΔF/F0
20s
ROIprocesses
50 ΔF/F0
20s
D
ROIsoma (ΔF/F0·s)
(11)
Control
TNFα
Recovery
ROIprocesses (ΔF/F0·s)
Control
TNFα
Recovery
E
Alexa 594
EGTA/
BAPTA
Alexa
488
20 μm
AstroEGTA internal
AstroBAPTA internal
TNFα
TNFα
10 pA
2s
10 pA
2s
F
AstroEGTA
mEPSC frequency (Hz)
(9)
TNFα
Time (s)
G
AstroBAPTA
mEPSC frequency (Hz)
(6)
TNFα
Time (s)

Figure 2

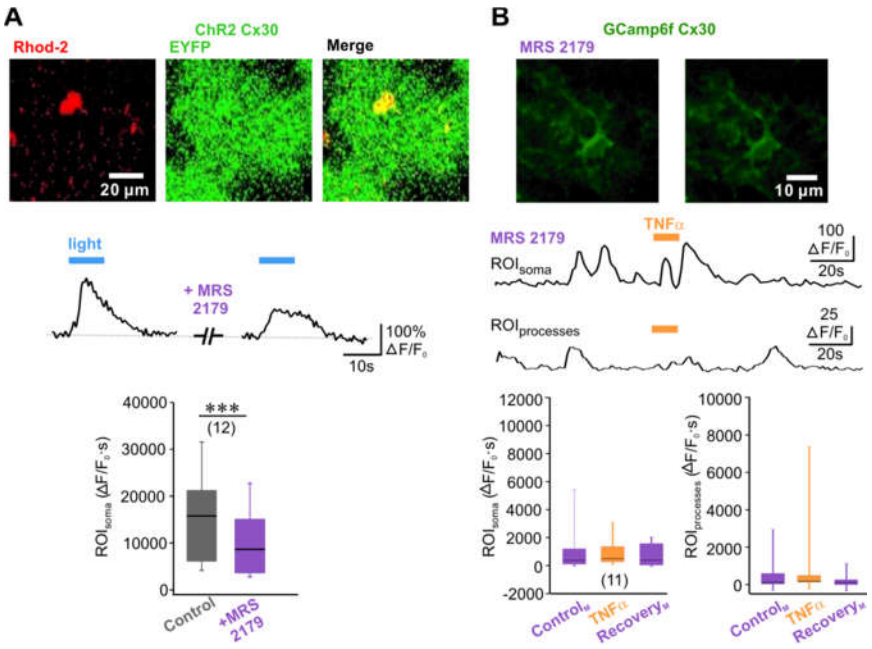
A
Rhod-2
ChR2 Cx30
EYFP
Merge
20 µm
light
+ MRS
2179
100%
ΔF/F0
10s
***
(12)
Control
+MRS
2179
B
GCamp6f Cx30
MRS 2179
10 µm
MRS 2179
TNFα
ROIsoma
100
ΔF/Fd
20s
ROIprocesses
25
ΔF/Fd
20s
(11)
Control
TNFα
Recovery

**Figure 3**

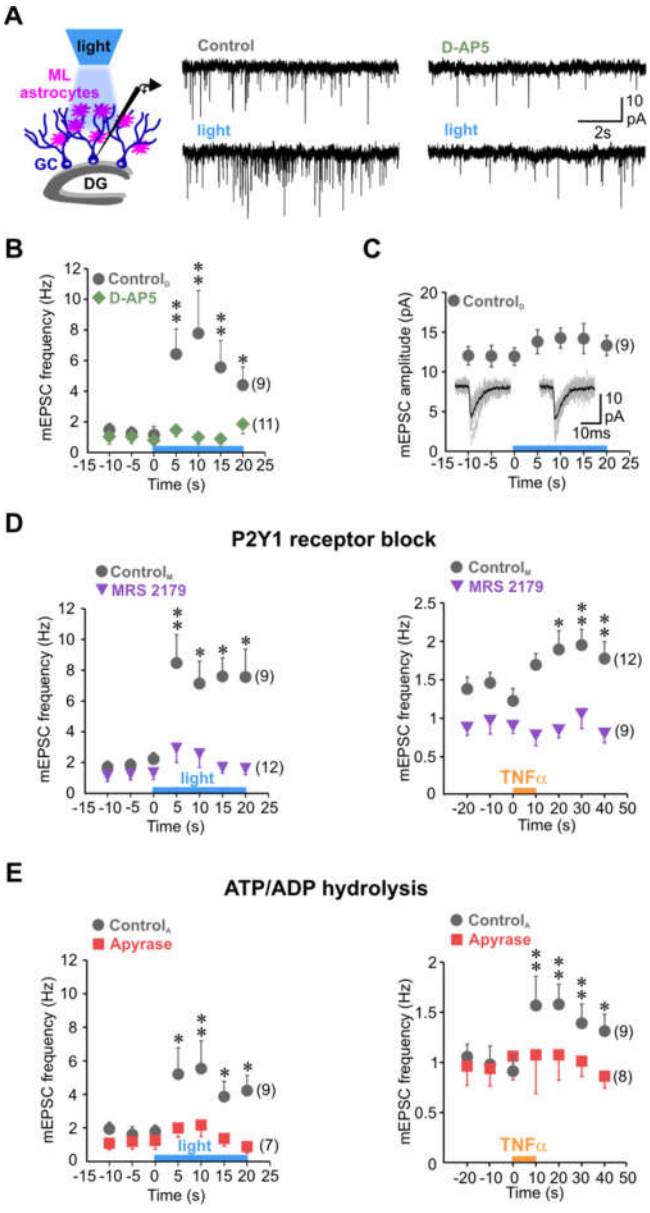
A
light
ML
astrocytes
GC
DG
Control
D-AP5
light
light
10
pA
2s
B
Control
D-AP5
mEPSC frequency (Hz)
(9)
(11)
Time (s)
C
Control
mEPSC amplitude (pA)
(9)
10
pA
10ms
Time (s)
D
P2Y1 receptor block
Control
MRS 2179
mEPSC frequency (Hz)
(9)
(12)
light
Time (s)
Control
MRS 2179
(12)
(9)
TNFα
Time (s)
E
ATP/ADP hydrolysis
Control
Apyrase
mEPSC frequency (Hz)
(9)
(7)
light
Time (s)
Control
Apyrase
(9)
(8)
TNFα
Time (s)

**Figure 4**

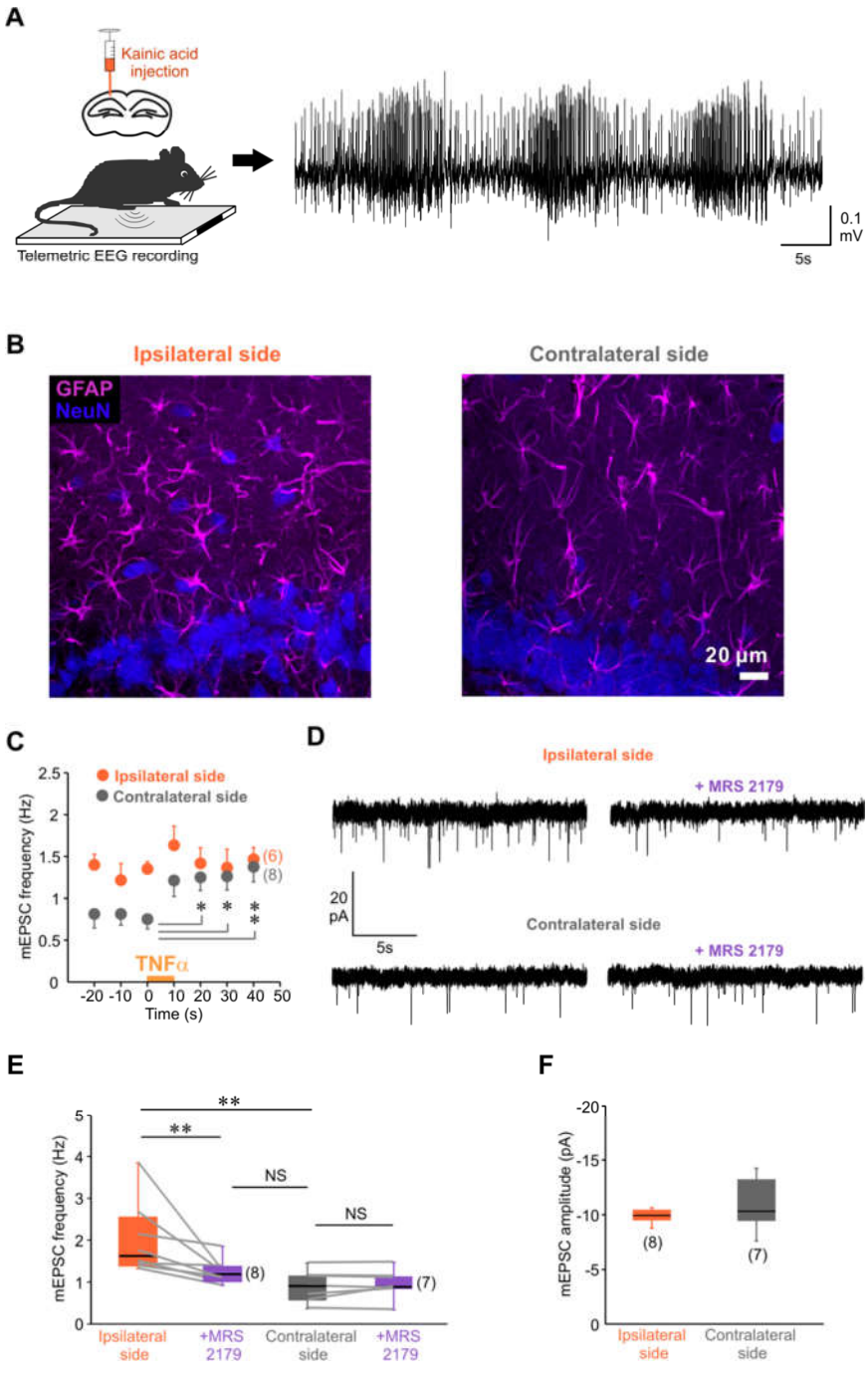
A
Kainic acid injection
Telemetric EEG recording
0.1 mV
5s
B
Ipsilateral side
Contralateral side
GFAP
NeuN
20 µm
C
Ipsilateral side
Contralateral side
mEPSC frequency (Hz)
(6)
(8)
TNFα
Time (s)
D
Ipsilateral side
+ MRS 2179
20 pA
5s
Contralateral side
+ MRS 2179
E
mEPSC frequency (Hz)
**
**
NS
NS
(8)
(7)
Ipsilateral side
+MRS 2179
Contralateral side
+MRS 2179
F
mEPSC amplitude (pA)
(8)
(7)
Ipsilateral side
Contralateral side

# Supporting Information

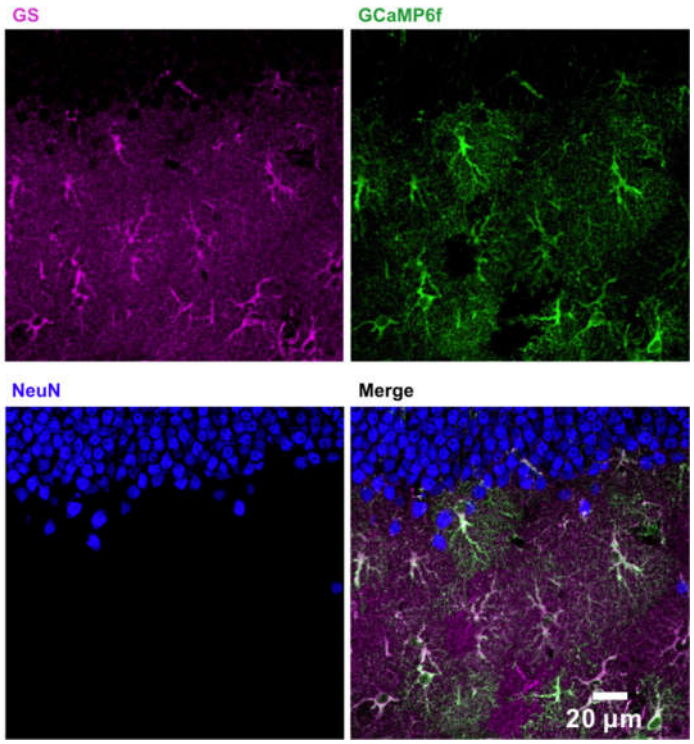


**Supporting Figure 1. Immunohistochemistry data showing specific GCaMP6f expression in the dentate gyrus astrocytes.**

Specific *GCaMP6f* expression in molecular layer astrocytes of a young adult *Cx30-CreERT2:GCaMP6f* mice. Z-projection of confocal images of the dentate gyrus labeled for astrocytes (glutamine synthetase, GS), neurons (NeuN) and *GCaMP6f* (GFP). No neurons were co-labeled with GFP whereas the soma and the processes of GS positive astrocytes were co-labelled with GFP.

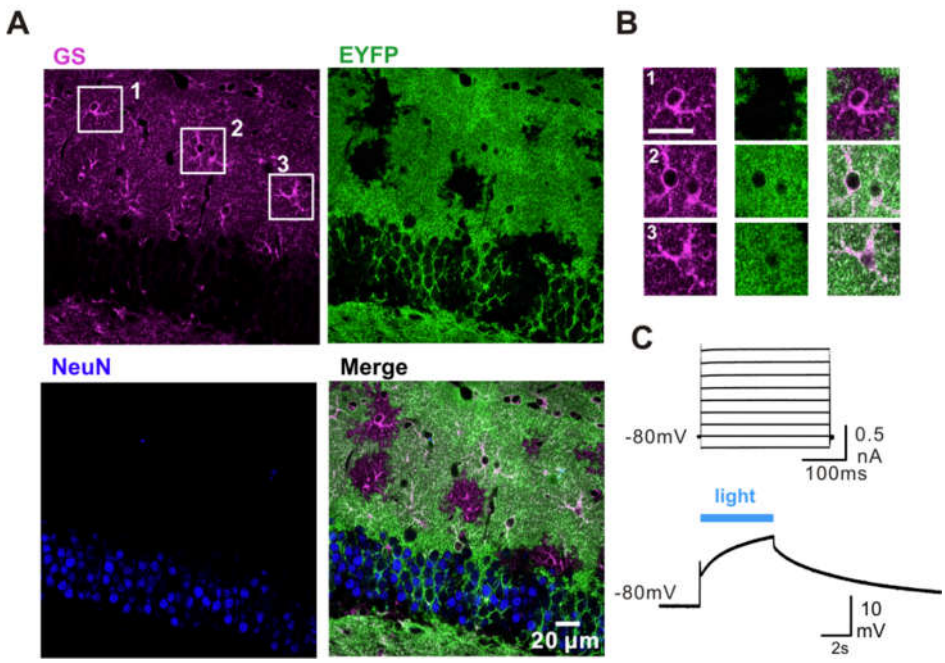


**Supporting Figure 2. Data showing selective ChR2 expression in astrocytes and control of astrocyte activity by blue light.**

(A) Expression of *ChR2* in *Cx30-CreERT2:ChR2-EYFP* young adult mouse. *ChR2-EYFP* expression is identified in a large proportion of molecular layer astrocytes labeled by glutamine synthetase (GS). *ChR2* expression is not detected in the layer of granule cells labeled with NeuN. (B) Enlarged view (single 0.5 µm optical slice) on astrocytes marked by rectangles in **a**: 1, EYFP-negative and 2, 3 EYFP-positive astrocytes. Scale bar 20 µm. (C) I-V curve in response to 20 mV depolarizing steps from –100 mV to +60 mV obtained from *ChR2-EYFP*-positive astrocyte illustrate typical passive membrane properties. Patch-clamp recording from an astrocyte expressing *ChR2* shows the change in the membrane potential that precisely follows the duration of the light pulse (blue rectangle).

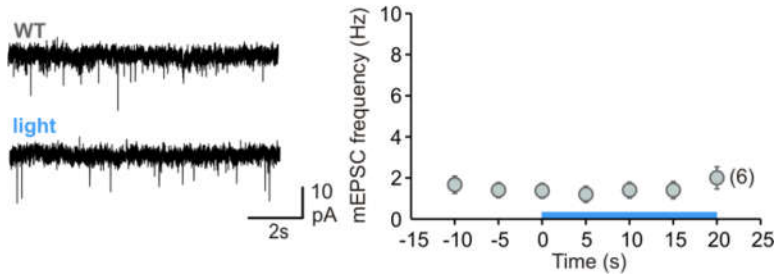


**Supporting Figure 3. Data showing the effect of light stimulation in wild-type mouse (WT).** Traces and summary graph show that blue light stimulation does not evoke any change in mEPSC frequency in WT mouse (n=6, 2 animals, p=0.26, One-way RM ANOVA on Ranks). Data are presented as mean±SEM.

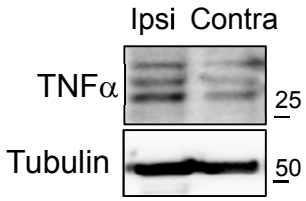


**Supporting Figure 4. Increase of TNFα in ipsilateral hippocampus 24h after unilateral intracortical kainate injection.**

Increase of TNFα in ipsilateral hippocampus 24 hr after unilateral intracortical kainate injection. Representative (1 out of 3 tested mice) western blotting analysis of ipsilateral and contralateral hippocampus extracts indicates a higher TNFα content in the ipsilateral hippocampus